




Investigation of sulfuric acid-treated activated carbon properties

Neda ASASIAN KOLUR^{1,*}, Seyedmehdi SHARIFIAN¹, Tahereh KAGHAZCHI²

¹Fouman Faculty of Engineering, College of Engineering, University of Tehran, Fouman, Iran

²Department of Chemical Engineering, Amirkabir University of Technology, Tehran, Iran

Received: 25.10.2018

Accepted/Published Online: 16.01.2019

Final Version: 03.04.2019

Abstract: A granulated type of commercial activated carbon (GAC) with surface area of 828 m²/g was treated with a strong solution of sulfuric acid (98% wt.) at a temperature of 30 °C. The physicochemical and porous properties and the surface chemistry of the sorbents were investigated and compared in detail. It was established that the lower temperatures of impregnation and the higher concentration of H₂SO₄ solution resulted in the introduction of higher percentages of sulfur-containing groups and smaller porosity loss. The results of EDS, FTIR, and XPS tests confirmed the introduction of sulfone groups and acidic oxygenated ones, which increased the adsorbent affinity towards mercury species available in the aqueous phase (pH 7) by 20%. It was found that acid-washing treatment helped to reduce the ash content of GAC and cleaned its internal space; however, with the introduction of bulky H₂SO₄ molecules into micropores and narrow mesopores of GAC, the surface area and pore volume were reduced. The increase of mercury adsorption capacity in spite of decreasing porosity after acid treatment shows that trapping in pores is not the only mechanism involved in mercury adsorption.

Key words: Activated carbon, sulfuric acid, acid treatment, characterization, mercury

1. Introduction

Activated carbons (ACs) generally consist of heteroatoms such as oxygen, nitrogen, and sulfur, which create surface functionalities if placed on the graphene plates' edges. Most of the surface functional groups give a hydrophilic character to the sorbent and have a major role in adsorbing various molecules from liquid and gaseous phases. Several oxygen-containing groups such as carboxyl, anhydrides, hydroxyls, lactones, and lactol groups give an acidic character to activated carbons. In contrast, chromene, pyrone, and quinones enhance the basicity of ACs.¹ Surface modification of adsorbents with changing/coverage of available groups, introduction of new chemicals, and changing hydrophilic character and acidity of adsorbents can promote or inhibit the chemical adsorption of special species on the adsorbent surface.

Sulfur can be introduced onto the AC surface as different forms of functional groups including mercaptan (thiol), sulfide, disulfide, sulfenic/sulfinic/sulfonic acid, sulfoxide, and sulfone. Elemental sulfur,² H₂S,³ SO₂,⁴ CS₂,⁵ DMDS,⁵ Na₂S, K₂S,⁶ etc. are some of the components that have been previously studied for sulfur introduction onto AC surfaces. In addition, the performance of sulfuric acid for modification of ACs has been studied by several researchers.^{7–12} To use the previous findings, a literature review was carried out and the results are classified in Table 1. It was observed that only a limited number of works focused on H₂SO₄ acid treatment as a posttreatment process on AC. The other works that used sulfuric acid as a chemical activating

*Correspondence: n.asasian@ut.ac.ir

agent for conversion of raw materials into activated carbons are not considered.^{13–16} The table provides the main information including the primary carbonaceous adsorbent to be treated, procedure of acid impregnation and operating conditions, changes in physical and chemical properties after modification, and applications of acid-treated adsorbents.

Several applications for H₂SO₄ treated ACs are investigated, such as adsorption of ammonia,⁸ VOC,¹⁰ and mercury¹² from gaseous and liquid phases. In addition, carbon-based sulfonated catalysts have become a research hotspot in recent years, and one of the most common sulfonation methods is the direct use of H₂SO₄.^{17–19} Gomes et al. worked on H₂SO₄ treatment of activated carbon to produce catalysts for catalytic wet peroxide oxidation of a model anionic azo dye.¹⁷ Acetylation of glycerol to biofuel additives, which was one of the other catalytic applications of sulfated activated carbons, was studied by Khayoon and Hameed.¹⁸ Mendoza used the catalytic effect of sulfuric acid treated AC in wet air oxidation of phenol.¹⁹

As noted in Table 1, several previous works have focused on the potential of H₂SO₄-treated ACs for removal of elemental mercury (Hg⁰) from aqueous and gaseous systems. After observing the better performance of virgin AC in adsorption of elemental mercury from flue gas in the presence of SO₂, O₂, and water vapor, H₂SO₄-treated ACs were identified as strong Hg⁰ adsorbents. SO₂ and O₂ react to produce SO₃, and sulfur trioxide is converted into H₂SO₄ in the presence of H₂O. Based on the work performed by Uddin et al., H₂SO₄ contributes to the Hg⁰ adsorption process according to the following reactions (Eqs. (1) and (2)):²⁰



Hg⁰ is first physically adsorbed on the surface of the carbonaceous adsorbent, and then it is oxidized either by physisorbed O₂ or by acidic C–O functional groups (usually available on the surface of carbonaceous adsorbents). The oxidation property of S(VI) (in the structure of sulfuric acid) may also help to give adsorbed Hg²⁺ or HgO.^{11,20,21} The enhanced Hg⁰ adsorption capacity is finally related to the higher solubility of oxidized Hg species in H₂SO₄.²¹ He et al. reported that the effect of H₂SO₄ on Hg⁰ adsorption capacity of carbonaceous sorbents depends on the combination of the concentration and charge of the SO₄ cluster.¹¹ Li et al. also used a H₂SO₄-treated AC for Hg⁰ removal from flue gas at 125 °C. The enhancement in Hg⁰ adsorption capacity after acid treatment was explained via the physisorption mechanism resulting from either the narrower microporosity or the increased surface polarity.²² The adsorption ability of H₂SO₄-treated activated carbons towards mercury species available in aqueous solutions was studied in a few works.¹²

The main aim of the present work is to study the physicochemical properties, surface functionalities, and porous characteristics of H₂SO₄-treated activated carbon and compare the results with the corresponding values for the untreated one. The adsorptive capacity of acid-treated activated carbon towards mercury species is also compared and explained in brief.

2. Results and discussion

2.1. Morphology, composition, and physicochemical properties

SEM micrographs are shown in Figure 1 for GAC and GAC-H₂SO₄. The cleaner surface of GAC-H₂SO₄ confirms that H₂SO₄ contributes in acid washing and helps to remove impurities and ash contents from the

Table 1. A literature review on the modification of ACs with H_2SO_4 for the use in adsorption applications.

Starting material and H_2SO_4 treatment procedure	Influence on functional groups	Influence on porosity	Application	Ref.
Outgassed AC was treated with H_2SO_4 solution (25%, 50% vol./vol. and concentrated H_2SO_4) under temperatures of 30, 50, and 70 °C for 2, 6, and 12 h	Oxygenated groups were changed, and sulfate and bisulfate were formed	Surface area and microporosity were decreased	-	7
AC fiber was immersed in hot aqueous solution of H_2SO_4	Sulfonyl groups (-SO) were formed	Surface area reduced and average pore diameter increased a little	Ammonia adsorption through growth of ammonium sulfate on the surface of adsorbent	8
AC wet oxidized in concentrated H_2SO_4 at temperatures between 150–270 °C	Carboxyls, phenols, and hydroxyl groups were formed	Mesoporous volume and specific surface areas were increased	Higher adsorption capacities for large molecules and less for small ones	9
Commercial AC was treated with H_2SO_4 solution with concentrations of 5 or 10 wt.%, for stirring time of 12 h	Surface oxygen group species were formed	Specific surface area was reduced and microporosity increased	Mixed VOC (benzene and toluene) removal from contaminated air	10
Commercial AC was treated with H_2SO_4 solution (5 and 40% vol./vol.) at temperatures of 25 and 140 °C for 24 h, after drying was heated up to 700 °C under N_2 flow for 2 h	Organic sulfur (thiol) was detected, oxygen surface groups were increased	Micropore volume increased a little, mesopore volume and specific surface area increased more significantly	Mercury removal in aqueous solutions	12
Commercial AC was treated with H_2SO_4 solution with concentration of 5.4 and 20.1% wt., and impregnation ratio of 1 g solid/1 mL solution	-	Pore blocking effect resulted from the presence of bulk H_2SO_4 phase within AC pores	Elemental mercury removal from air and aqueous solutions	21
Commercial AC was treated with H_2SO_4 solution (50% wt.) at 25 fC for 20 h	-	Microporous volume decreased but mesoporous volume remained constant	Hg^0 removal from flue gas	22

GAC structure. Although the figure cannot predict the exact influence of acid-washing treatment on the pores' geometry, the opening of the large cavities' mouths and pore widening are evident from SEM micrographs.

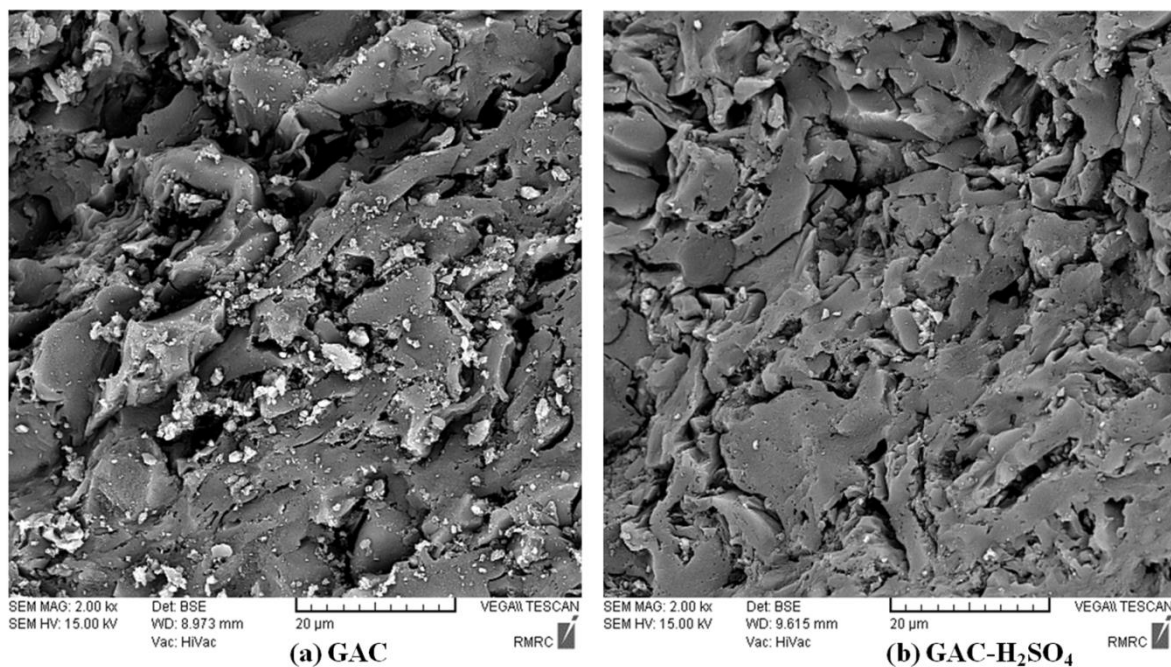


Figure 1. SEM micrographs of (a) GAC and (b) GAC-H₂SO₄.

Some of the physicochemical properties of GAC in comparison with GAC-H₂SO₄ are presented in Table 2. The loss of ash percentage after acid treatment is in accordance with the SEM observations. Acid treatment did not have any significant impact on the average size and hardness of the particles; however, the bulk density of GAC decreased a little after acid treating.

Table 2. The physicochemical properties of GAC and GAC-H₂SO₄.

Properties	GAC	GAC-H ₂ SO ₄
Particle diameter (mm)	0.853–1.20	0.853–1.20
Bulk density (g/cm ³)	0.47	0.42
Ball-pan hardness (%)	95	95
Ash content (%)	7	4

The results of EDS analysis are also given in Table 3. EDS results show a decrease in the percentages of heteroatoms (such as Si and N) after acid washing. However, the surface sulfur content is increased a little. This confirmed that the H₂SO₄ washing process removes silica-containing compounds and other impurities from the matrix of activated carbon and introduces sulfur onto the surface.

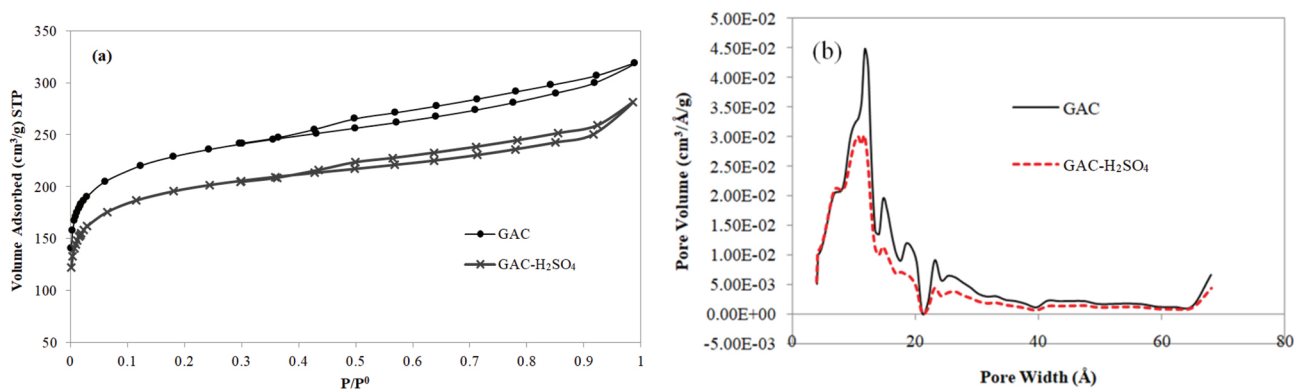
2.2. Porosity studies

Figures 2a and 2b respectively show the N₂ adsorption-desorption isotherms and DFT pore size distributions of both samples. Both sorbents show relatively similar isotherms and PSDs, with a little shift towards lower adsorbed nitrogen volumes for GAC-H₂SO₄. Table 4 shows that the overall porosity of GAC is decreased during

Table 3. The weight percentages of different elements on the surfaces of sorbents (hydrogen atoms cannot be detected using SEM-EDS).

Elements	Weight percentages of surface elements	
	GAC	GAC-H ₂ SO ₄
C	84.3	85.5
N	2.4	2.1
O	12.0	10.6
S	0.4	1.1
H	-	-
Al	0.1	0.3
Si	0.8	0.4

H₂SO₄ impregnation; the values of BET surface area and total pore volume decrease from 828 m²/g and 0.55 cm³/g to 620 m²/g and 0.45 cm³/g, respectively, after acid treatment. Reduction of porosity and surface area after impregnation of adsorbents with external chemicals (such as H₂SO₄) is not unexpected, especially if the modification process occurs at relatively low temperatures. Such behavior was previously observed for H₂SO₄ treatment in several works (Table 1).^{7,8} The main reason for this behavior is the blockage of the mouths of micropores/narrow mesopores with bulky impregnating molecules. Fine pores have the main role in increasing the surface area of sorbents, and thus their blockage leads to a limited surface area. Remaining large mesopores and their widening because of oxidation of the edges of the carbonaceous matrix shift the pore size distribution curve of the acid-treated sorbent towards larger average pore widths and increase the average mesopore widths (Table 4).¹⁹

**Figure 2.** Comparison of (a) N₂ adsorption-desorption isotherms and (b) DFT pore size distribution of the adsorbent samples.

The review of the literature shows that surface area loss after impregnation is not a general rule, and there are a few works that reported an increase in the specific surface area after H₂SO₄ treatment, such as the one carried out by Jiang et al. at a temperature of 250 °C. The sample treated at 250 °C showed an increase of 86% in mesopore volume and 90% in surface area, which enhanced the adsorption capacity of sorbent towards large molecules like methylene blue and dibenzothiophene.⁹ Mendoza also used sulfuric acid treatment for preparation of a catalyst for catalytic wet air oxidation of phenol. For the sulfuric acid wash, the carbon

Table 4. The porous properties of GAC and H₂SO₄-impregnated GAC.

Porous properties	GAC	GAC-H ₂ SO ₄
BET specific surface area (m ² g ⁻¹)	828	620
Total pore volume (cm ³ g ⁻¹)	0.55	0.45
Average pore width (Å) (4 V _{tot} /S _{BET})	26.5	29.1
Micropore volume (HK method) (cm ³ g ⁻¹)	0.39	0.30
Mesopore volume (BJH desorption) (cm ³ g ⁻¹)	0.17	0.13
External surface area (t-method) (m ² g ⁻¹)	212.2	132.7
Average micropore width (HK method) (Å)	8.0	8.0
Average mesopore width (BJH desorption) (Å)	31.9	32.2

sample was boiled for 1 h in 96% wt. H₂SO₄ with weight ratio of 9:1 acid to dried AC. An important increase of the mesopore volume and a small increase in the surface area and micropore volume were observed.¹⁹ In another work carried out by Abdelouahab Reddam et al., H₂SO₄ treatment (at a relatively low temperature) was followed by a post-heat treatment process under nitrogen flow at 700 °C for 2 h. They also reported a small increase of BET surface area and porous volume, probably related to the additional heat treating step.¹²

2.3. FTIR results

The chemical nature of surface functionalities is investigated using FTIR and XPS tests. Figure 3 compares FTIR spectra of both samples; the broad peak that appeared around the wavenumber of 3430 cm⁻¹ in both spectra is related to the stretching vibration of O-H. The weak peaks occurring near 2850 and 2920 cm⁻¹ also represent the aliphatic C-H stretching vibrations. C=C stretching vibrations result in weak peaks near 1630 cm⁻¹. C-C skeletal and C-H out-of-plane deformation lead to vibrations near 798 cm⁻¹ for both adsorbents.²³ One broad strong stretching vibration representing C-O bonds in alcohols can be observed at 1090 cm⁻¹, for GAC; this peak shifts a little and appears around 1120 cm⁻¹ for GAC-H₂SO₄, representative of the sulfone groups introduced into the surface of treated adsorbent.¹⁵ Sulfate and bisulfate ions give rise to two bands usually located in the ranges of 1080–1130 and 610–680 cm⁻¹.⁷ A peak at 617 cm⁻¹ can also be seen in the spectra of GAC-H₂SO₄. At lower wavenumbers around 511 and 466 cm⁻¹, several weak peaks are found for GAC, attributed to Si-C stretching vibrations stemming from the silicon-containing ash contents in the bituminous coal structure.²³ Such vibrations are not found for the acid-treated AC. The typical bulk chemical composition of bituminous coal is as follows: C: 55.67%, H: 38.57%, N: 0.73%, O: 4.96%, and S: 0.07% wt., with ash content of 4.86%, which contains Si, Al, etc.²⁴

2.4. XPS results

Figure 4 shows the C_{1s} spectra of the adsorbents. Based on the positions of the deconvoluted peaks and the areas under each curve, the percentages of different kinds of carbon bonds are determined (Table 5).^{25,26} C_{1s} signals are composed of five constituents; the second peak (which appeared between 285.3 and 285.7 eV) corresponds to the carbon present in phenolic, alcohol, ether, C=N groups, or C-S bonds. The percentage of these kinds of carbons on the surface of GAC-H₂SO₄ is lower than GAC. The presence of the C-S bond on the surface of GAC may originate from the structure of bituminous coal used for preparation of GAC. Reduction of

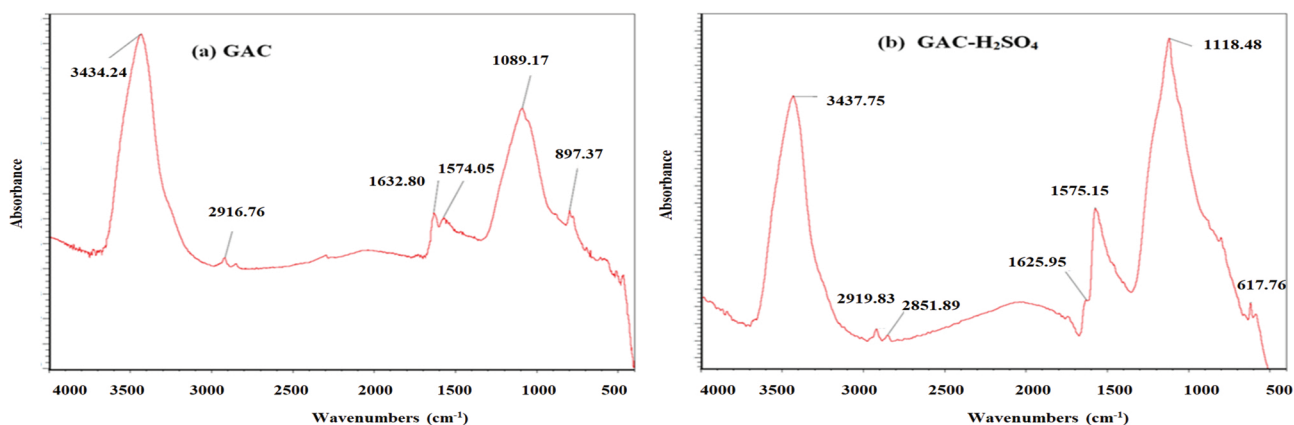


Figure 3. FTIR spectra of (a) GAC in comparison with (b) GAC-H₂SO₄.

all kinds of organic oxygen (carbon-oxygen bonds) may be representative of converting such groups into sulfur-oxygen groups or probably covering the surface with sulfone groups. The higher contribution of graphitic carbon in GAC-H₂SO₄ reflects the ash-removal ability of H₂SO₄, which increases the percentage of the remaining C-C and C-H bonds on the surface of this sample.

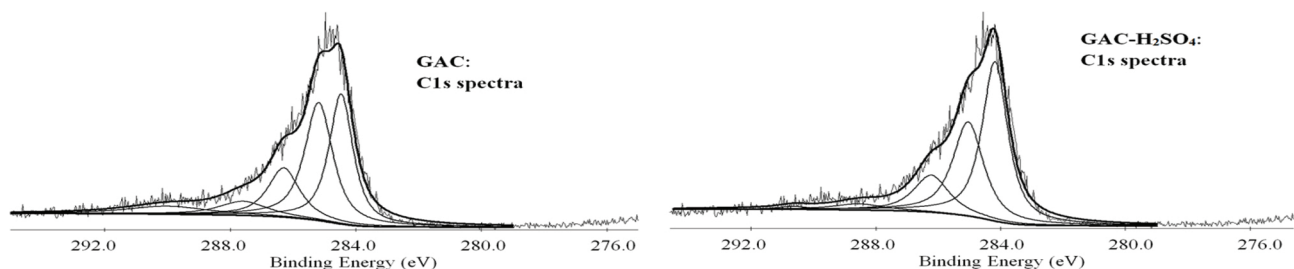


Figure 4. C_{1s} spectra of GAC and GAC-H₂SO₄.

Table 5. Distribution of atomic percentage of carbon on the surface of GAC and GAC-H₂SO₄.

	Graphitic carbon	Carbon present in phenolic, alcohol, ether, C=N groups, or C-S bonds	Carbonyl or quinone groups (C=O)	Carboxyl or ester groups (C=O)	Shake-up satellite peaks due to π - π^* transitions in aromatic systems
Binding energy (eV)	284.0–284.3	285.3–285.7	286.8–287.4	288.5–289.2	290.2–291.1
GAC	35.51	35.34	16.59	7.42	7.13
GAC-H ₂ SO ₄	47.08	33.21	15.00	3.65	1.06

Figure 5 shows the O_{1s} spectra for both samples, and Table 6 presents the contribution of each kind of atomic oxygen. Oxygen is found in three forms in GAC, including C=O, C-O, and chemisorbed oxygen or H₂O;^{27,28} however, for GAC-H₂SO₄, a new peak related to the oxidized form of sulfur (S-O) can be observed (binding energy: 531.2 eV).²⁹ For this sample, approximately 8.59% of the oxygen atoms are bound with sulfur.

The higher percentage of chemisorbed water on the surface of GAC- H_2SO_4 is related to the hydrogen bonding property of sorbent promoted by H_2SO_4 trapped in the pores of the sample. Similar behavior was previously observed by Li et al.²¹

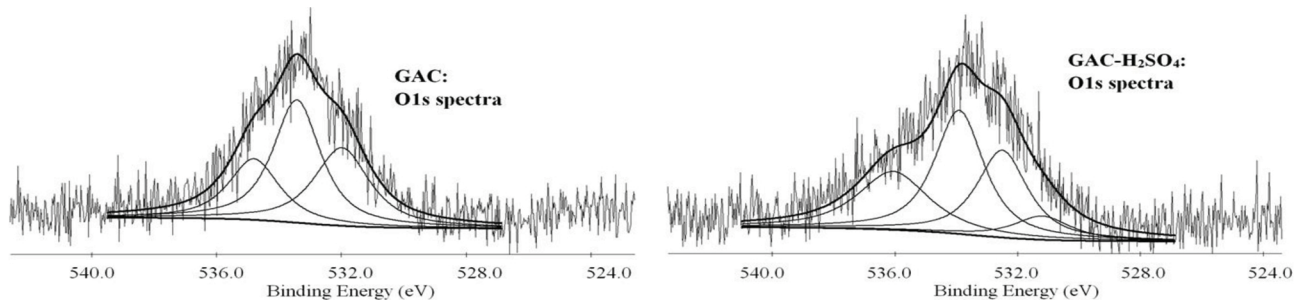


Figure 5. O_{1s} spectra of GAC and GAC- H_2SO_4 .

Table 6. Distribution of atomic percentage of oxygen on the surface of GAC and GAC- H_2SO_4 .

	Oxidized sulfur (O-S)	Oxygen double bonded to carbon (O=C)	Oxygen single bonded to carbon (C-O)	Chemisorbed oxygen and/or water
Binding energy (eV)	531.2	531.5–532.5	533–534	534.8–536
GAC	-	32.72	43.88	23.40
GAC- H_2SO_4	8.59	27.57	37.96	25.88

Finally, Figure 6 shows the XPS spectra in the S_{2p} region for both adsorbents to compare sulfur bonds. The spectrum of GAC- H_2SO_4 shows a distinct peak around 168 eV; the appearance of such a peak at binding energies over 167 eV confirms the formation of oxidized forms of sulfur (sulfone group).³⁰ The smaller peak in the spectrum of GAC around 164 eV is related to the organic sulfur structures resulting from the nature of primary coal.

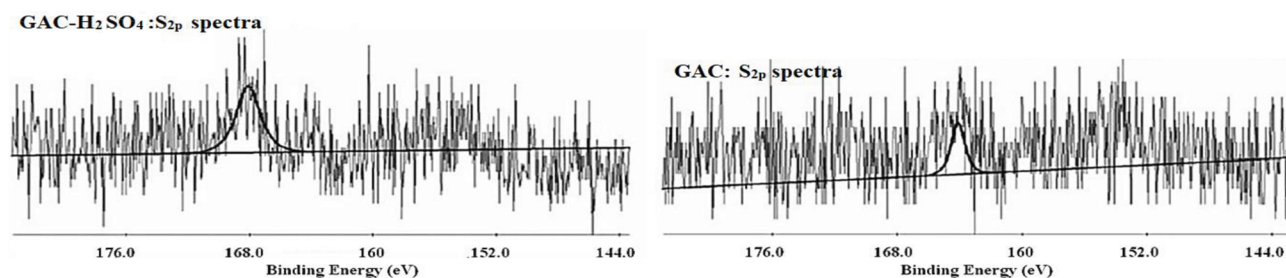


Figure 6. S_{2p} spectra of GAC and GAC- H_2SO_4 .

Among many different reactions that may be involved in the acid-treatment process, one of the main reactions is the one that introduces sulfone groups onto the surface of GAC. For the purpose, HSO_3^+ can be generated by protonation of a sulfuric acid molecule with another one and then breaking off the water molecule. It results in the formation of sulfonium ion (HSO_3^+). HSO_3^+ can react with the aromatic rings of graphene plates

(available in the AC structure) or some of the functional groups located on the edges, by attacking/sharing electrons to create new bonds. The protons released may then transfer back to the solution.³¹

2.5. pH_{pzc} analysis

Figure 7 shows the results of pH_{pzc} measurement for GAC and GAC- H_2SO_4 comparatively. The primary GAC with an alkaline character (pH_{pzc} 8.75) changed into a strong acidic sorbent (pH_{pzc} 2.5) after H_2SO_4 treatment. This is in confirmation with a previous study.⁸ Normally it is expected that the adsorption of cationic heavy metal ions like Hg^{2+} is promoted when the pH of the solution is larger than pH_{pzc} , since the adsorbent surface has a negative charge under these conditions. Therefore, the acid treatment of GAC extends the appropriate pH range for adsorption of cationic species. However, this property may not be so determining for mercury adsorption, where stronger interactions other than the electrostatic forces are probably involved. Generally, it is very simplistic to suppose that mercury species are entirely available in cationic form in aqueous solutions. Metal cations are usually found in complex with ligands in solutions, depending on the type of side anions present in solution, and of course this can be distinguished by the use of species distribution modeling. Figure 8 shows that at basic and acidic pH levels, the dominant species are respectively $\text{Hg}(\text{OH})_2$ and HgCl_2 .^{5,32}

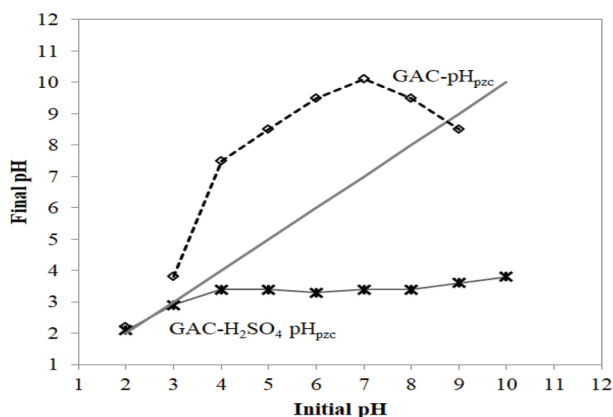


Figure 7. The diagram of pH_{pzc} measurement for GAC and GAC- H_2SO_4 .

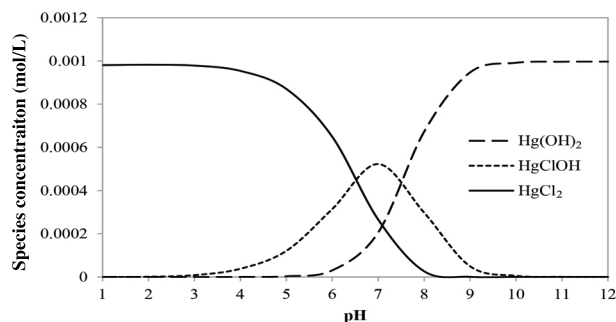


Figure 8. Mercury speciation in a 200 mg/L mercury(II) solution prepared from dissolution of HgCl_2 in H_2O .

2.6. Mercury adsorption results

Mercury adsorption capacities of GAC and GAC- H_2SO_4 under each combination of conditions were measured and shown in Table 7. Comparison of the adsorption capacities and removal percentages obtained by both sorbents (runs 1 and 2) demonstrates the higher affinity of GAC- H_2SO_4 towards mercury. It can be seen that mercury adsorption capacity after H_2SO_4 treatment increased from 100 to 144.33 mg/g at pH 7 and temperature of 30 °C. The increase of mercury adsorption capacity in spite of decreasing porosity of the sorbent after acid treatment (Table 4) shows that trapping in pores is not the only mechanism involved in mercury adsorption. The larger adsorption capacity of acid-treated GAC is related to the presence of sulfone and acidic oxygenated groups on the surface of sorbent. From the economical and practical viewpoint, improving the mercury uptake percentage of the adsorbent (by approximately 20%) through such a cost-effective and easy procedure is a great success.

Table 7. Affinity of GAC and GAC-H₂SO₄ toward mercury adsorption from aqueous solutions.

Run	Adsorbent	Adsorption conditions		Hg adsorption capacity (mg/g)	Adsorption percentage (%)
		Initial pH of solution	Temperature (°C)		
1	GAC	7	30	100.00	50.00
2	GAC-H ₂ SO ₄	7	30	141.33	70.67
3	GAC-H ₂ SO ₄	10	30	60.01	30.00
4	GAC-H ₂ SO ₄	7	50	151.22	75.61
5	GAC-H ₂ SO ₄	10	50	104.73	52.36

The effect of initial pH of solutions on the adsorption capacity of GAC-H₂SO₄ was also determined (runs 2 and 3 at 30 °C, and runs 4 and 5 at 50 °C). The lower affinity of GAC-H₂SO₄ towards mercury at high pH levels is attributed to the higher solubility of hydroxyl complexes of mercury (Hg(OH)₂), which are the dominant species in this pH range. Comparison of runs 2 and 4 and runs 3 and 5 shows the influence of temperature on the mercury adsorption capacity of GAC-H₂SO₄. In both cases, higher temperature helps to increase the mercury adsorption capacity. This represents the endothermic nature of stages involved in mercury adsorption (such as cation dehydration, film and intraparticle diffusion, desorption of H₂O molecules from the adsorbent's sites for substituting with mercury species, complexation with sulfone and oxygenated groups, etc.).

H₂SO₄ as a sulfur-containing oxidizing agent can be used for producing sulfonated activated carbon through a simple, cost-effective, and energy-saving impregnation procedure. To reach a larger amount of sulfur-containing groups and lower porosity limitations, H₂SO₄ impregnation should be performed at low temperatures (room temperature) with higher concentrations (98% wt.). The presence of sulfone species and acidic oxygen-containing groups on the surface of GAC-H₂SO₄ was confirmed by the results of FTIR and XPS tests. Silica and other impurities available in the structure of GAC that stem from the bituminous coal structure were eliminated by H₂SO₄ treatment. The low temperature treatment of GAC with H₂SO₄ caused surface area limitation and porosity loss due to the blockage of fine pores' mouths and oxidation of the edges of the carbonaceous matrix. However, because of the more significant role of surface chemistry than porosity, mercury adsorption capacity of GAC-H₂SO₄ was 20% greater than that of GAC at 30 °C and initial pH 7.

3. Experimental

3.1. Sulfuric acid treatment of AC

The primary adsorbent was commercial GAC provided by Jacobi Carbons Company, prepared from steam activation of bituminous coal. GAC modification was performed based on a simple impregnation method at 30 °C. Five grams of GAC was contacted with 200 mL of strong solution of sulfuric acid (98% wt.) in a shaker-incubator shaking at the speed of 200 rpm at 30 °C for 12 h. GAC-H₂SO₄ was washed several times with sufficient volume of distilled water at 80 °C under thorough stirring (each step lasted for 1 h). After each step, the washing solution was separated from the adsorbent by filtration and the pH of the solution (filtrate) was measured. During the first steps of washing, the pH of the filtrate was strongly acidic, but after several steps, it reached the pH of distilled water. After that, no matter how long the washing process continued, the pH of the filtrate remained constant. The washing process was thus continued until achieving a constant washing pH. The samples were finally oven-dried at 100 °C for 6 h.

3.2. Choosing the appropriate modification conditions

The most appropriate operating conditions for acid treatment of GAC were chosen based on the results of previous studies. To the knowledge of the authors, the most influential factors on the modification (impregnation) of sorbents are the temperature and concentration of acid solution, and, to a lesser extent, the impregnation time. The influence of these factors on the BET surface area and porosity of sorbents and also the amounts of surface sulfur-containing functional groups have been studied in some previous works. Gomes et al. investigated the effect of different concentrations (5–18 M) of sulfuric acid solution and temperature of treatment (80–150 °C) on the concentration of sulfur groups, surface acidity, and porosity of AC. Comparison of the adsorbents' properties showed that the increase of molarity is in favor of making higher concentrations of sulfur groups (including thiol and sulfone) on the surface of AC sample. At higher temperatures for all concentrations, the amounts of sulfone and thiol groups decrease significantly. On the other hand, the increase of H₂SO₄ concentration is beneficial to porosity development; however, at high concentrations, increasing the temperature reduces the specific surface area and micropore volume.^{17,33} Abdelouhab Reddam et al. also investigated the effect of H₂SO₄ solution concentration (5% and 40% vol./vol.) and temperature (25 and 140 °C) on the treatment performance. In this procedure, after moderate stirring of the suspension for 24 h, a post-heat treatment under nitrogen flow at 700 °C for 2 h was performed. The results of TPD and XPS tests showed that the treated samples exhibited sulfur-containing groups only when the temperature of impregnation was 25 °C (lower level) and a higher level of H₂SO₄ concentration was applied. It is established that the presence of surface sulfur improves the mercury removal capacity of the adsorbent; however, the smaller influence of textural properties and oxygen-containing surface groups should be recognized.¹² Therefore, it seems that larger concentrations and lower temperatures are the best operating conditions for acid treatment of AC for the aim pursued in this work.

The effect of acid-treatment temperature at very higher levels (150–225 °C) was also investigated by Ven Pelt.³⁴ It was found that H₂SO₄ treatment under temperatures around 150 °C leads to introduction of carboxylic, phenolic, and lactonic groups, and for higher temperatures, the values of acidic groups decrease. Briefly, concentrated H₂SO₄ only behaves as an oxidizing agent if the system is heat-treated at high temperatures below its boiling point (around 300 °C). Therefore, in order to obtain a sulfonated AC with large capacity towards mercury, H₂SO₄ treatment should be performed with concentrated H₂SO₄ solution (98% wt. ≈ 18 M) under ambient temperature (30 °C).

3.3. Characterization of adsorbents

The measurement of bulk density, ash content, and hardness of the sorbents was carried out according to standard methods; the details can be found elsewhere.^{5,35} FTIR analysis was carried out to investigate the surface functionalities of the sorbents using a Nicolet spectrometer (NEXUS 670) on pellets prepared from the powdered adsorbents combined with KBr as the carrier. The infrared spectra were recorded in the wavenumber region of 4000 to 400 cm⁻¹ plotted on the absorbance axis. The XPS data were gathered using a VG Microtech instrument consisting of a XR3E2 X-ray source, a twin anode (Mg K α and Al K α), and a concentric hemispherical analyzer. The powdered samples were first inserted into the ultrahigh vacuum chamber (10⁻⁷ mbar). The XPS data were evaluated using an XPS peak fitting program (XPSPEAK41) in three regions of survey (C, O, and S). The presence of C, N, S, O, and other impurities (Al and Si) on the surface of sorbents was evaluated using a TESCAN model VEGAI fitted with EDS microanalysis. SEM micrographs were also gathered to evaluate and compare the morphology of the samples. N₂ physical adsorption-desorption

measurement at $-196\text{ }^{\circ}\text{C}$ was performed using an automatic volumetric apparatus (Quantachrome NOVA 1000) after degassing of the samples at $110\text{ }^{\circ}\text{C}$ for 4 h. The BET equation, HK, and BJH (desorption data) methods were applied to calculate the specific surface area, micropore, and mesopore distribution, respectively, using Autosorb software.³⁶ The pH drift method was applied for measuring the pH of zero charge (pH_{pzc}). Several samples of KNO_3 solutions (50 mL and 0.1 M) with different initial pH values (in the range of 1 to 12) were mixed with 0.10 g of adsorbents; the suspensions were shaken for 48 h at room temperature. Plotting the final pH values versus the initial ones gives pH_{pzc} as the point where these two values are equal.³⁷

3.4. Mercury adsorption experiments

The stock solution (1000 mg/L Hg(II)) was prepared by dissolving 1.354 g of HgCl_2 (Merck) in 10 mL of HNO_3 solution (Merck, 65% wt.) and then reaching a volume of 1 L with deionized water. Acidification of the stock solution prevents precipitation of mercury at such high concentrations. Measurement of mercury concentration in aqueous solutions before and after adsorption was performed using an atomic absorption spectrophotometer (Varian AA240). Prior to the measurement, acidification of the samples was performed using concentrated nitric acid to assure that mercury elimination only resulted from adsorption, not precipitation. It is necessary to mention that the present work only intends to compare the affinity of virgin activated carbon and a sulfuric acid-treated one towards mercury. Thus, the precise study of mercury adsorption kinetics, equilibrium, and thermodynamics by both sorbents is not the subject of this work. A limited number of experiments were carried out to investigate the influence of pH and temperature on the adsorption percentage. In this regard, mercury solutions (50 mL, initial Hg(II) concentration 200 mg/L, and initial pH 7 and 10) were agitated (shaking speed of 200 rpm) in contact with adsorbents (dosage of 0.05 g/50 mL solution) at two different temperatures (30 and 50 $^{\circ}\text{C}$) for 24 h to assure equilibrium. Each run was performed at least two times under identical conditions to assure the reproducibility of experimental results (maximum 5% error).

References

1. Ania, C. O.; Bandosz, T. J. In *Activated Carbon Surfaces in Environmental Remediation*; Bandosz, T. J., Ed. Elsevier: Oxford, UK, 2006, pp. 159-230.
2. Asasian, N.; Kaghazchi, T. *Sep. Sci. Technol.* **2013**, *48*, 2059-2072.
3. Feng, W.; Kwon, S.; Feng, X.; Borguet, E.; Vidic, R. D. *J. Environ. Eng.* **2006**, *132*, 292-300.
4. Asasian, N.; Kaghazchi, T.; Faramarzi, A.; Hakimi-Siboni, A.; Asadi-Kesheh, R.; Kavand, M.; Mohtashami, S. A. *J. Taiwan Inst. Chem. Eng.* **2014**, *45*, 1588-1596.
5. Asasian, N.; Kaghazchi, T. *Ind. Eng. Chem. Res.* **2012**, *51*, 12046-12057.
6. Ranganathan, K.; Balasubramanian, N. *Eng. Life Sci.* **2002**, *2*, 127-129.
7. Gomez-Serrano, V.; Acedo-Ramos, M.; López-Peinado, A. J. *J. Chem. Tech. Biotechnol.* **1997**, *68*, 82-88.
8. Kim, K. H.; Shin, C. S. *Carbon Sci.* **2001**, *2*, 109-112.
9. Jiang, Z.; Liu, Y.; Sun, X.; Tian, F.; Sun, F.; Liang, C.; You, W.; Han, C.; Li, C. *Langmuir* **2003**, *19*, 731-736.
10. Pak, S. H.; Jeon, M. J.; Jeon, Y. W. *Int. Biodeterior. Biodegrad.* **2016**, *113*, 195-200.
11. He, P.; Wu, J.; Jiang, X.; Pan, W.; Ren, J. *Surf. Rev. Lett.* **2014**, *21*, 1450018.
12. Abdelouahab Reddam, Z.; Wahby, A.; El Mail, R.; Silvestre-Albero, J.; Rodríguez Reinoso, F.; Sepúlveda-Escribano, A. *Adsorpt. Sci. Technol.* **2014**, *32*, 101-115.
13. Karagöz, S.; Tay, T.; Ucar, S.; Erdem, M. *Bioresour Technol.* **2008**, *99*, 6214-6222.

14. Mashhadi, S.; Javadian, H.; Ghasemi, M.; Saleh, T. A.; Gupta, V. K. *Desalin. Water Treat.* **2016**, *57*, 21091-21104.
15. Adibfar, M.; Kaghazchi, T.; Asasian Kolor, N.; Soleimani, M. *Chem. Eng. Technol.* **2014**, *37*, 979-986.
16. Jawad, A. H.; Rashid, R. A.; Ishak, M. A. M.; Wilson, L. D. *Desalin. Water Treat.* **2016**, *57*, 25194-25206.
17. Gomes, H. T.; Miranda, S. M.; Sampaio, M. J.; Silva, A. M. T.; Faria, J. L. *Catal. Today* **2010**, *151*, 153-158.
18. Khayoon, M. S.; Hameed, B. H. *Bioresource Technology* **2011**, *102*, 9229-9235.
19. Mendoza, M. B. PhD, Rovira i Virgili University, Tarragona, Spain, 2008.
20. Uddin, M. A.; Yamada, T.; Ochiai, R.; Sasaoka, E.; Wu, S. *Energy Fuels* **2008**, *22*, 2284-2289.
21. Morris, E. A.; Kirk, D. W.; Jia, C. Q.; Morita, K. *Environ. Sci. Technol.* **2012**, *46*, 7905-7912.
22. Li, Y. H.; Serre, S. D.; Lee, C. W.; Gullett, B. K. In *EPA/DOE/EPRI MegaSymposium 2001, Proceedings of the U.S. EPA/DOE/EPRI Combined Power Plant Air Pollutant Control Symposium, and the Air & Waste Management Association Specialty Conference on Mercury Emissions: Fate, Effects, and Control*; Chicago, IL, USA, 20-23 August 2001.
23. Pavia, D. L.; Lampman, G. M.; Kriz, G. S.; Vyvyan, J. A. *Introduction to Spectroscopy*; Brooks Cole: Belmont, CA, USA, 2008.
24. Kurková, M.; Klika, Z.; Martinec, P.; Pěgřimočová, J. *Bull Geosci.* **2003**, *78*, 23-34.
25. Laszlo, K.; Josepovits, K.; Tombacz, E. *Anal. Sci.* **2001**, *17*, 1741-1744.
26. Boehm, H. P. *Carbon* **2002**, *40*, 145-149.
27. Park, S. J.; Jung, W. Y. *J. Colloid Interface Sci.* **2002**, *250*, 93-98.
28. Biniak, S.; Szymanski, G.; Siedlewski, J.; Swiatkowski, A. *Carbon* **1997**, *35*, 1799-1810.
29. Chulliyote, R.; Hareendrakrishnakumar, H.; Raja, M.; Gladis, J. M.; Stephan, A. M. *Chemistry Select* **2017**, *2*, 10484-10495.
30. Hsi, H. C.; Rood, M. J.; Rostam-Abadi, M.; Chen, S.; Chang, R. *Environ. Sci. Technol.* **2001**, *35*, 2785-2791.
31. Katritzky, A. R.; Kim, M. S.; Fedoseyenko, D.; Widyan, K.; Siskin, M.; Francisco, M. *Tetrahedron* **2009**, *65*, 1111-1114.
32. Dunham-Cheatham, S.; Farrell, B.; Mishra, B.; Myneni, S.; Fein, J. B. *Chem. Geol.* **2014**, *373*, 106-114.
33. Gomes, H. T.; Miranda, S. M.; Sampaio, M. J.; Figueiredo, J. L.; Silva, A. M. T.; Faria, J. L. *Appl. Catal. B* **2011**, *106*, 390-397.
34. Ven Pelt, A. H. MSc, Georgia Institute of Technology, Atlanta, GA, USA, 2012.
35. Kaghazchi, T.; Asasian Kolor, N.; Soleimani, M. *J. Ind. Eng. Chem.* **2010**, *16*, 368-374.
36. Lowell, S.; Shields, J. E.; Thomas, M. A.; Thommes, M. *Characterization of Porous Materials and Powders: Surface Area, Pore Size and Density*; Springer: Dordrecht, the Netherlands, 2004.
37. Smiciklas, I. D.; Milonjic, S. K.; Pfenndt, P.; Raicevic, S. *Sep. Purif. Technol.* **2000**, *18*, 185-194.